



OPEN ACCESS

EDITED BY

Jianxiang Chen,
Hangzhou Normal University, China

REVIEWED BY

Dingli Song,
First Affiliated Hospital of Xi'an Jiaotong
University, China
Muthukumar Rajasekaran,
National Cancer Centre Singapore,
Singapore

*CORRESPONDENCE

Guangjun Shi,
sgjzp@hotmail.com

SPECIALTY SECTION

This article was submitted to Cancer
Genetics and Oncogenomics,
a section of the journal
Frontiers in Genetics

RECEIVED 11 August 2022

ACCEPTED 20 October 2022

PUBLISHED 10 November 2022

CITATION

Jin Z, Song M, Wang J, Zhu W, Sun D,
Liu H and Shi G (2022), Integrative
multiomics evaluation reveals the
importance of pseudouridine synthases
in hepatocellular carcinoma.
Front. Genet. 13:944681.
doi: 10.3389/fgene.2022.944681

COPYRIGHT

© 2022 Jin, Song, Wang, Zhu, Sun, Liu
and Shi. This is an open-access article
distributed under the terms of the
[Creative Commons Attribution License
\(CC BY\)](https://creativecommons.org/licenses/by/4.0/). The use, distribution or
reproduction in other forums is
permitted, provided the original
author(s) and the copyright owner(s) are
credited and that the original
publication in this journal is cited, in
accordance with accepted academic
practice. No use, distribution or
reproduction is permitted which does
not comply with these terms.

Integrative multiomics evaluation reveals the importance of pseudouridine synthases in hepatocellular carcinoma

Zhipeng Jin¹, Mengying Song², Jianping Wang¹, Wenjing Zhu³,
Dongxu Sun¹, Huayuan Liu⁴ and Guangjun Shi^{4*}

¹Graduate School of Dalian Medical University, Dalian, China; Department of Hepatobiliary Surgery, Qingdao Municipal Hospital, Qingdao, China, ²Department of Operation Room, Cancer Hospital of Dalian University of Technology, Liaoning Cancer Hospital and Institute, Shenyang, China, ³Clinical Research Center, Qingdao Municipal Hospital, Qingdao, China, ⁴Department of Hepatobiliary Surgery, Qingdao Municipal Hospital, Qingdao, China

Background: The pseudouridine synthases (PUSs) have been reported to be associated with cancers. However, their involvement in hepatocellular carcinoma (HCC) has not been well documented. Here, we assess the roles of PUSs in HCC.

Methods: RNA sequencing data of TCGA-LIHC and LIRI-JP were downloaded from the Cancer Genome Atlas (TCGA) and the International Cancer Genome Consortium (ICGC), respectively. GSE36376 gene expression microarray was downloaded from the Gene Expression Omnibus (GEO). Proteomics data for an HBV-related HCC cohort was obtained from the CPTAC Data Portal. The RT-qPCR assay was performed to measure the relative mRNA expression of genes in clinical tissues and cell lines. Diagnostic efficiency was evaluated by the ROC curve. Prognostic value was assessed using the Kaplan-Meier curve, Cox regression model, and time-dependent ROC curve. Copy number variation (CNV) was analyzed using the GSCA database. Functional analysis was carried out with GSEA, GSVA, and clusterProfiler package. The tumor microenvironment (TME) related analysis was performed using ssGSEA and the ESTIMATE algorithm.

Results: We identified 7 PUSs that were significantly upregulated in HCC, and 5 of them (*DKC1*, *PUS1*, *PUS7*, *PUSL1*, and *RPUSD3*) were independent risk factors for patients' OS. Meanwhile, the protein expression of *DKC1*, *PUS1*, and *PUS7* was also upregulated and related to poor survival. Both mRNA and protein of these PUSs were highly diagnostic of HCC. Moreover, the CNV of *PUS1*, *PUS7*, *PUS7L*, and *RPUSD2* was also associated with prognosis. Further functional analysis revealed that PUSs were mainly involved in pathways such as genetic information processing, substance metabolism, cell cycle, and immune regulation.

Conclusion: PUSs may play crucial roles in HCC and could be used as potential biomarkers for the diagnosis and prognosis of patients.

KEYWORDS

pseudouridine synthase, HCC, biomarker, tumor microenvironment, multiomics data

Introduction

Hepatocellular carcinoma remains a global health challenge as one of the most malignant malignancies (Llovet et al., 2021). Early diagnosis and clinical intervention, together with advances in surgical methods and the development of anti-tumor therapies, have led to significant advances in the treatment of HCC. However, median survival time for patients with advanced HCC is only 2–3 years (Yang et al., 2019). Even in early HCC cases suitable for surgery, the 5-year recurrence rate after hepatectomy is close to 70% (Roayaie et al., 2013). The high heterogeneity of HCC is a massive challenge to improving clinical outcomes. Hence, there is an urgent need to explore the complex functional pathways and molecular mechanisms behind HCC, to develop new biomarkers for early diagnosis, prognosis and relapse prediction, and to identify new therapeutic targets (Llovet et al., 2018).

Post-transcriptional modifications could affect RNA stability, localization, structure, splicing, or function (Roundtree et al., 2017). And its deregulation has been linked to human diseases, including tumorigenesis (Jonkhout et al., 2017). RNA modifications regulate cancer cell fate by modulating cell survival, differentiation, migration and drug resistance (Delaunay and Frye, 2019). Pseudouridine (5-ribosyluracil, ψ) is the 5-ribosyl isomer of uridine, and is the most abundant type of RNA modification. It is also known as the ‘fifth nucleotide’ (Charette and Gray, 2000). Enzymes responsible for this modification are pseudouridine synthase (PUS). A total of thirteen PUSs have been identified in humans and are classified into two categories, RNA-dependent and RNA-independent PUSs (Supplementary Table S1). Of these, Dyskerin, the only RNA-dependent PUS, is a nucleolar protein encoded by the Dyskerin Pseudouridine Synthase 1 (*DKC1*) gene. It is present in small nucleolar ribonucleoprotein particles and is responsible for converting specific uridine residues of ribosomal (r) RNA into pseudouridine. And twelve RNA-independent PUSs can modify target RNAs by directly recognising sequences or RNA structures (Li et al., 2016).

Pseudouridine in cancer cells has emerged as a therapeutic target for cancer (Nombela et al., 2021). A recent study found that *DKC1* was a potential therapeutic target in colorectal cancer, and its increased expression was associated with poor prognosis (Kan et al., 2021). PUS7 was a targetable regulator of glioblastoma growth (Zhang et al., 2021a), and its increased expression was associated with reduced patient survival. The application of PUS7 inhibitors inhibited tumorigenesis and prolonged the life span of tumor-bearing mice (Cui et al., 2021). In ovarian cancer, both mRNA and protein expression of PUS7 were higher in cancer tissues than in normal tissues (Li

et al., 2021). All these emerging findings showed the potential of PUSs as cancer biomarkers. Therefore more research is necessary to explore the importance of PUSs in cancer.

Currently, there is a lack of research on PUSs in HCC. To address this scientific gap, we integrated transcriptomic, genomic and proteomic data to assess the diagnostic, prognostic and therapeutic value of PUSs and to preliminarily explore the potential mechanisms by which PUSs affect HCC.

Materials and methods

The flow chart for this study is shown in Figure 1.

Dataset sources and processing

Three transcriptomic datasets were analyzed in this study. The TCGA-LIHC (RNA sequencing in FPKM format) cohort, containing 50 adjacent samples and 374 HCC samples, was downloaded from GDC Data Portal (<https://portal.gdc.cancer.gov/>). The LIRI-JP (RNA sequencing in FPKM format) cohort, containing 202 adjacent samples and 243 HCC samples, was downloaded from ICGC Data Portal (<https://dcc.icgc.org/>). FPKM values were converted to TPM values for subsequent analyses. Mutation data and clinical data for TCGA-LIHC and LIRI-JP were derived from the same sources as the corresponding expression data. GSE36376 (standardized expression data) cohort, containing 193 adjacent samples and 240 HCC samples, was downloaded from the GEO database (<http://www.ncbi.nlm.nih.gov/geo/>). The GPL10558 platform file was used as a reference for gene annotation. The average expression of probes was used as the expression value of the gene matched to multiple probes. Expression data for GSE36376 were eligible for direct analysis. The original proteomics and clinical data for an HBV-related HCC cohort (ID: PDC000198) were downloaded from CPTAC Data Portal (<https://pdc.cancer.gov/pdc/>). The data preprocessing process and the normalized proteomics matrix were obtained from Gao’s study. (Gao et al., 2019). And a total of 6,478 proteins in 159 paired samples were included in subsequent analyses.

Public online bioinformatics databases

Gene Set Cancer Analysis (GSCA) is a comprehensive database for genomic and immunogenomic cancer analysis (<http://bioinfo.life.hust.edu.cn/GSCA/#/>) (Liu et al., 2018). Using the GSCA database, we analyzed CNV data from the TCGA-LIHC cohort, including the composition of CNV, the

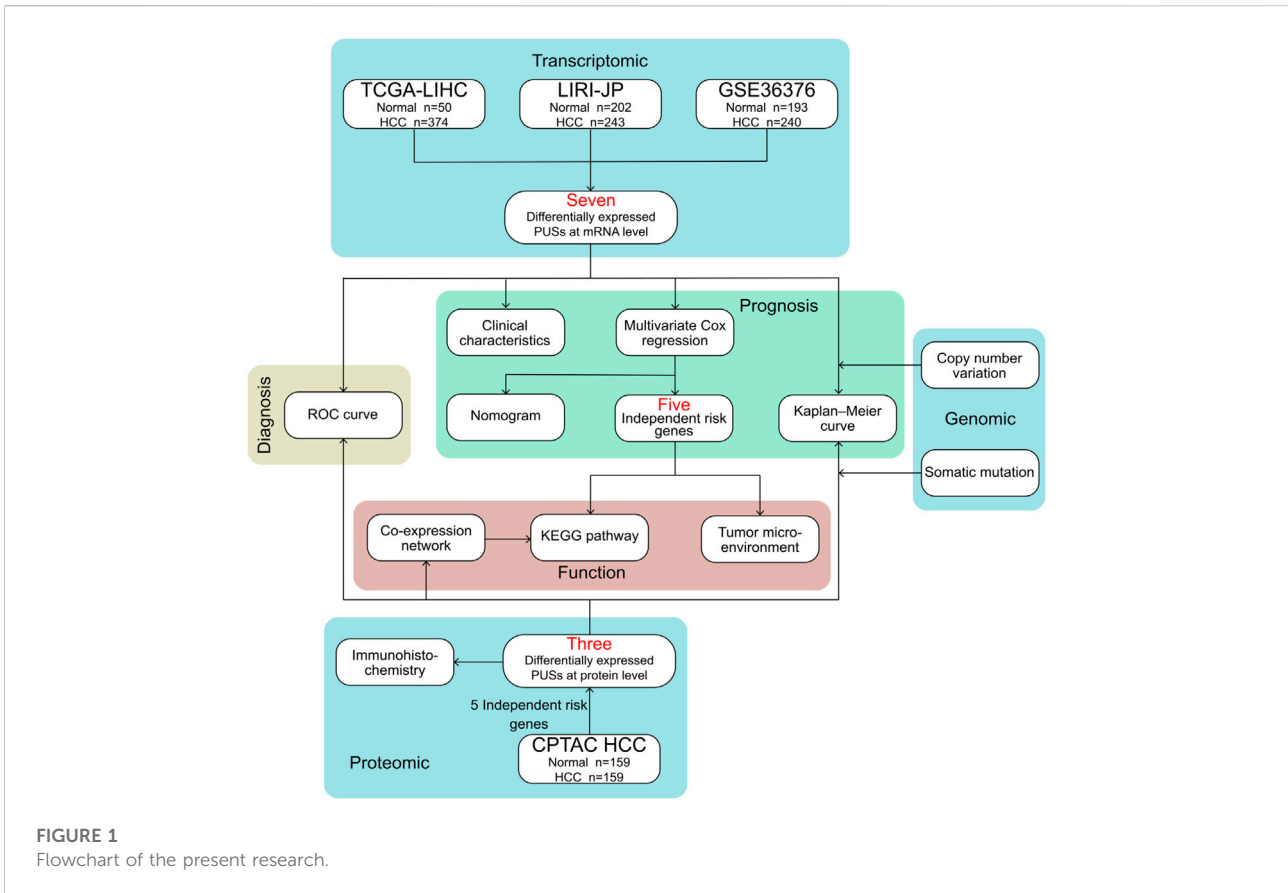


FIGURE 1
Flowchart of the present research.

correlation between copy number and gene expression, and the differences in survival of patients with different types of CNV.

The Human Protein Atlas (HPA) is an open-access resource for human proteins (<https://www.proteinatlas.org/>) (Uhlén et al., 2015). In our study, we assessed the expression levels of PUSs in clinical specimens and obtained several representative immunohistochemical staining results from the HPA database.

Functional and pathway enrichment analysis

Gene set enrichment analysis (GSEA) was used to identify KEGG pathways related to PUSs in HCC tissues (Subramanian et al., 2005). The annotation file (c2.cp.kegg.v7.5.1.symbols.gmt) was obtained from the MSigDB (<http://www.gsea-msigdb.org/gsea/downloads.jsp>). The analysis was performed using GSEA software (V4.2.1), and the number of permutations was set to 1,000. A false discovery rate (FDR) < 0.05 was considered a significant pathway enrichment. Gene set variation analysis (GSVA) was used to estimate the activity of KEGG pathways in each HCC sample (Hänzelmann et al., 2013). The GSEABase

package was used to read pathway information, and the GSVA package was used to convert the gene expression matrix into a gene set score matrix. Moreover, the clusterProfiler package was used to identify and visualize the GO terms (including biological process, cellular component, and molecular function) and KEGG pathways enriched for proteins.

Correlation of PUSs with tumor microenvironment

A previous study conducted an extensive immunogenomic analysis of over 10,000 tumor samples from 33 different cancer types in the TCGA and identified six immune subtypes spanning cancer tissue types (Thorsson et al., 2019). In our study, we analyzed the differences in PUSs expression in samples of different immune subtypes from the TCGA-LIHC cohort. The abundance of different immune cell types and the activity of immune functional pathways in HCC samples were estimated by single sample gene set enrichment analysis (ssGSEA) (Barbie et al., 2009). The analysis was performed using the GSEABase package and the GSVA package. The ESTIMATE algorithm could score tumor purity, the level of stromal cells, and the

level of immune cell infiltration in the tumor tissue based on expression data (Becht et al., 2016). We obtained stromal score, immune score, ESTIMATE score, and tumor purity for HCC samples using the estimate package.

Collection of the clinical specimens

The clinical specimens involved in this study were obtained from HCC patients who underwent hepatectomy at Qingdao Municipal Hospital. All patients had been pathologically confirmed and diagnosed with HCC. Cancer tissues and matched paracancerous tissue were frozen immediately in liquid nitrogen after resection and then stored at -80°C prior to use. The study was approved by the Ethics Committee of the Qingdao Municipal Hospital and conducted following the Declaration of Helsinki.

Cell culture

Human hepatocyte LO2 cells and human HCC cells (Hep3B, Huh7) were purchased from the Chinese Academy of Sciences Cell Bank (Shanghai, China). The cells were cultured in Dulbecco's modified Eagle's medium (DMEM; HyClone, United States) containing 10% fetal bovine serum (FBS; Excellbio, United States) and 1% penicillin - streptomycin (HyClone, United States). All cells were incubated at 37°C under 5% CO_2 .

RNA extraction and quantitative real-time PCR

Total RNA was extracted from clinical tissues or cell lines with TRIzol reagent (Tiangen Biotech, China). cDNA was synthesized from total RNA using a PrimeScript RT reagent kit (TaKaRa). SYBR Green assays (TaKaRa) were used to perform the RT-qPCR. *GAPDH* was used as the loading control, and the $2^{-\Delta\Delta\text{Ct}}$ method was used to calculate the relative expression of mRNA. The primer sequences are listed in Supplementary Table S2.

Statistical analysis

Statistical analyses were performed using R software (V4.1.2). Comparisons between two groups and multiple groups were presented via Wilcoxon rank-sum test and the Kruskal-Wallis test, respectively, unless otherwise specified. ROC curves were performed to measure the specificity and sensitivity of the variables for the diagnosis of HCC. Spearman correlation test was adopted to ascertain the correlation between variables. K-M survival curve and the log-rank test were utilized to compare survival differences between groups of patients. The optimal cut-off for groups was determined using the *survminer* package.

Univariate and multivariate COX regression was used to perform independent prognostic analysis and to construct a prognostic model. The optimal model was identified based on the Akaike information criterion (AIC). The nomogram was based on the independent prognostic factors filtered by multivariate Cox analysis and generated using the rms package. The predictive performance of the nomogram was evaluated by time-dependent ROC curves and calibration curves. Throughout the analysis, three multivariate COX analyses were performed, which were used for the independent prognostic analysis of single PUS, the construction of the PUS score and the construction of the nomogram, respectively. $p < 0.05$ was considered statistically significant.

Results

mRNA expression and diagnostic value of PUSs in hepatocellular carcinoma

First, we analyzed the mRNA expression levels of 13 PUSs in two RNA-seq datasets (Supplementary Table S3). As shown in Figures 2A,B, PUSs expression was generally higher in HCC tissues than in non-cancerous tissues. In the TCGA-LIHC cohort, the expression of *DKC1*, *PUS1*, *PUS3*, *PUS7*, *PUS7L*, *PUSL1*, *RPUSD1*, *RPUSD2*, *RPUSD3*, *RPUSD4*, *TRUB1*, and *TRUB2* was upregulated in HCC tissues. While there was no difference in the expression of *PUS10* (Figure 2C). In the LIRI-JP cohort, *DKC1*, *PUS1*, *PUS7*, *PUS7L*, *PUSL1*, *RPUSD1*, *RPUSD2*, *RPUSD3*, *RPUSD4*, *TRUB1*, and *TRUB2* were upregulated in HCC tissues, and *PUS10* was downregulated. In addition, the expression of *PUS3* in HCC did not differ from that in non-cancerous tissues (Figure 2D). Next, we calculated the fold change (mean TPM in HCC/mean TPM in normal samples) for each gene and set fold change >1.5 as the threshold. As a result, nine genes were screened in the TCGA-LIHC cohort and seven in the LIRI-JP cohort. Of these, a total of seven genes (*DKC1*, *PUS1*, *PUS7*, *PUSL1*, *RPUSD1*, *RPUSD2*, and *RPUSD3*) met the condition in both cohorts, and we considered them as DEGs (Figure 2E). Then, we validated the expression of DEGs using the GSE36376 cohort, and the trends were consistent with the previous results (Figure 2F). Finally, we evaluated the diagnostic value of DEGs at the mRNA level using ROC curves. As shown in Figure 2G, these genes were of high diagnostic value in all three HCC cohorts (AUC 0.798–0.977).

In summary, we identified 7 PUSs that were significantly upregulated in HCC tissues, which may be closely related to HCC and could be used as biomarkers for HCC diagnosis.

Correlation between PUSs expression and clinicopathological parameters

Here, we analyzed the correlation of PUSs expression with two important clinicopathological parameters, tumor stage

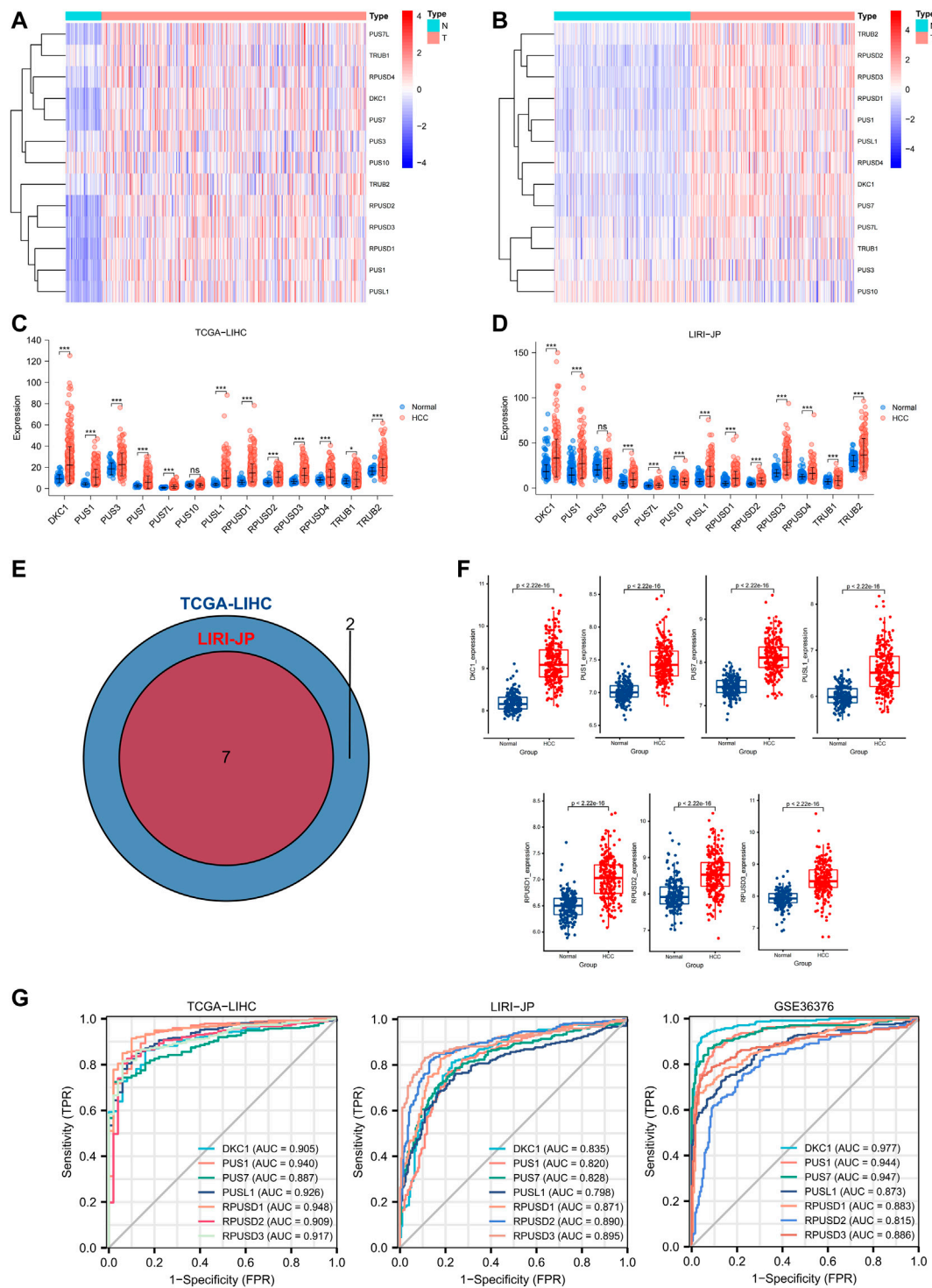
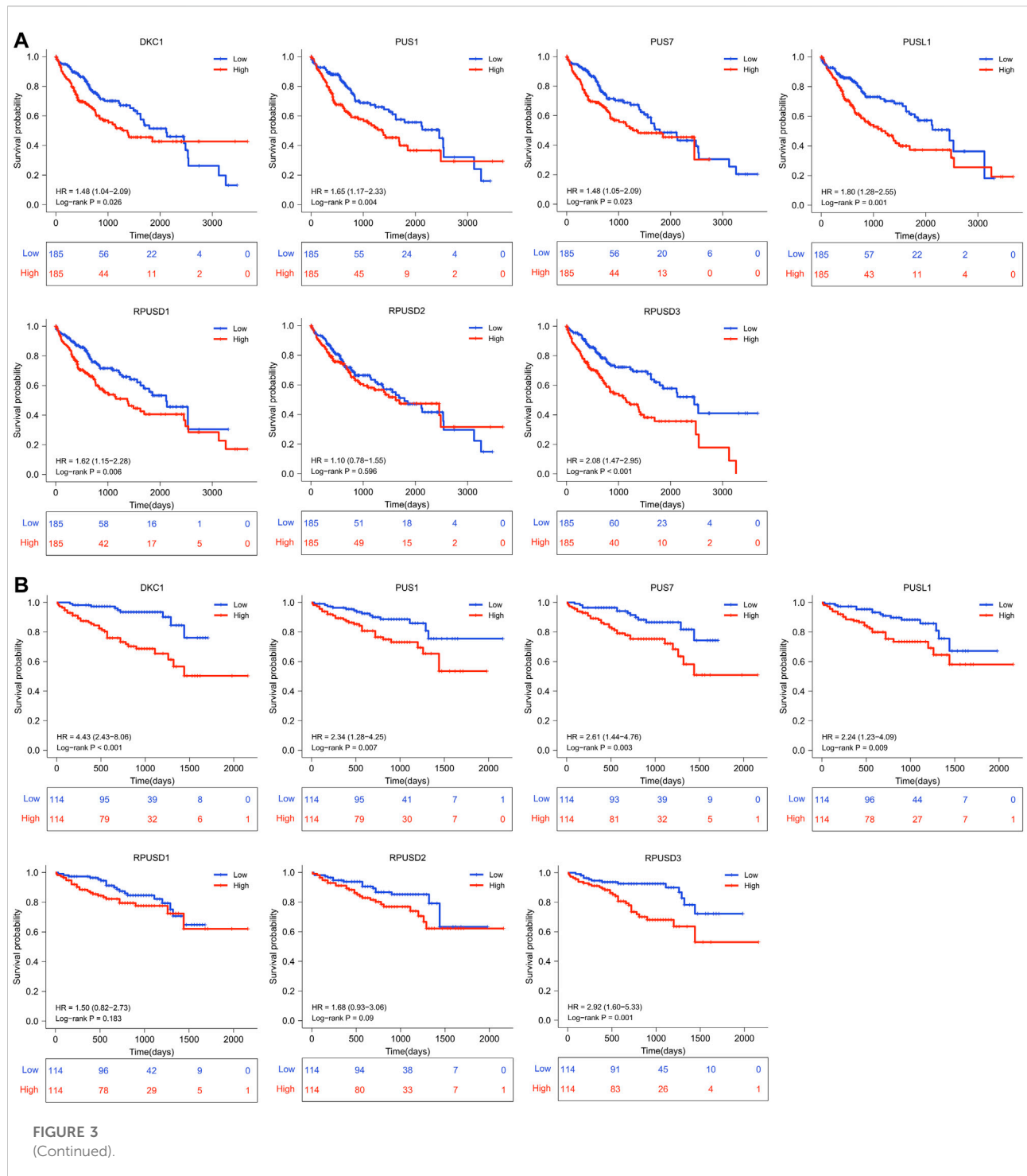


FIGURE 2

Expression profile and diagnostic value of *PUSs* mRNA in HCC. (A–B) Heatmap of *PUSs* expression in TCGA-LIHC (A) and LIRI-JP (B); (C–D) Expression difference of *PUSs* between non-cancerous tissues and HCC in TCGA-LIHC (C) and LIRI-JP (D); (E) Venn diagram of differentially expressed *PUSs* between non-cancerous tissues and HCC in TCGA-LIHC and LIRI-JP; (F) Expression of seven differentially expressed *PUSs* between non-cancerous tissues and HCC in GSE36376; (G) ROC curves of *PUSs* expression in three HCC cohorts. (ns: no statistical significance, * $p < 0.05$, ** $p < 0.01$, and *** $p < 0.001$).



and tumor grade. As shown in [Supplementary Figure S1A](#), in the TCGA-LIHC cohort, all the DEGs had higher expression levels in poorly differentiated tissues than in well-differentiated tissues. In the ICGC cohort, due to incomplete and inaccurate information about tumor grade, we only included part of the samples in the analysis. The

results showed that, except for RPUSD2, the median expression of the other six PUSs was higher in poorly differentiated tissues than in well-differentiated tissues ([Supplementary Figure S1B](#)). Notably, the results for PUS7, RPUSD2 and RPUSD3 were not statistically significant, which may be due to the small sample size of poorly differentiated

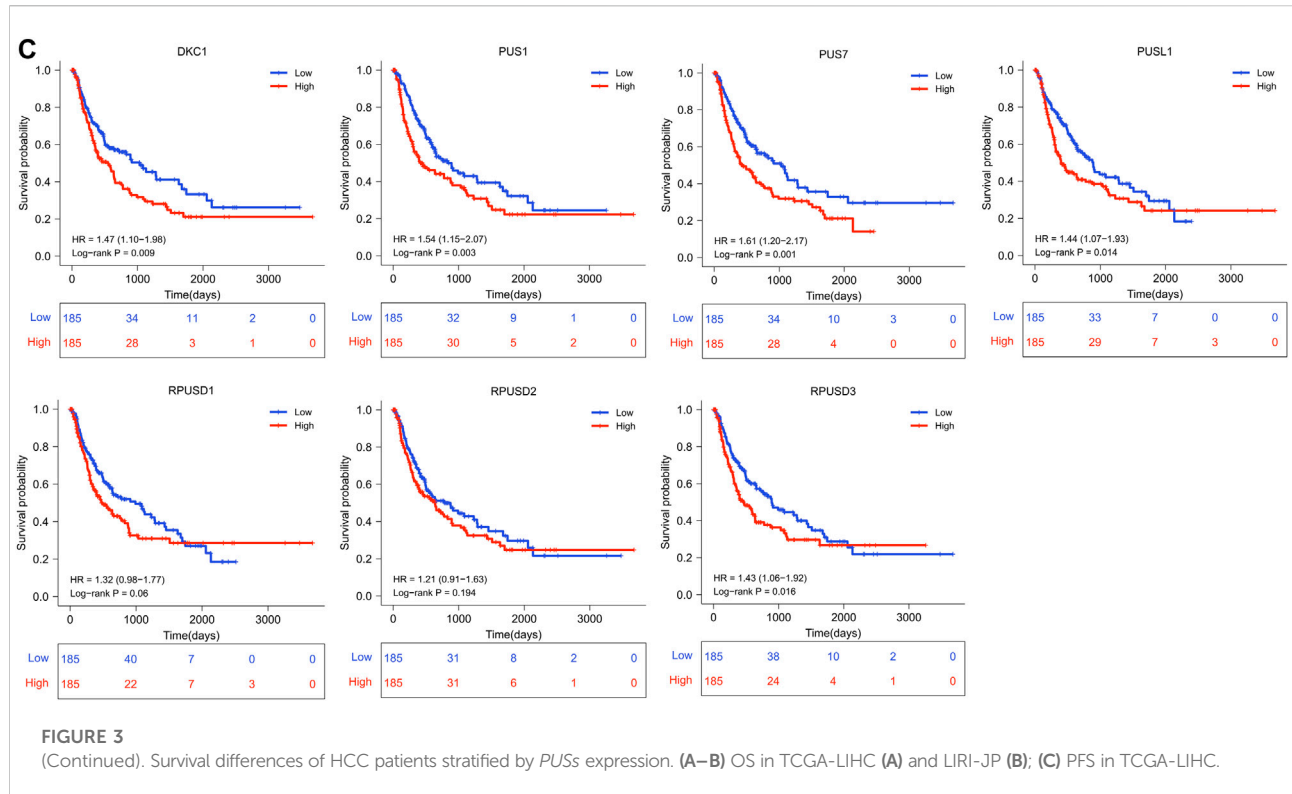


TABLE 1 Univariate Cox analysis of *PUSs* and clinical factors.

Characteristics	Univariate analysis				Progression Free Survival (PFS)	
	Overall Survival (OS)				TCGA-LIHC	
	TCGA-LIHC		LIRI-JP		TCGA-LIHC	
	HR (95% CI)	P	HR (95% CI)	P	HR (95% CI)	P
DKC1	1.021(1.012-1.031)	<0.001	1.022(1.014-1.030)	<0.001	1.012(1.004-1.021)	0.003
PUS1	1.054(1.030-1.080)	<0.001	1.023(1.008-1.039)	0.003	1.037(1.015-1.060)	0.001
PUS7	1.061(1.027-1.097)	<0.001	1.073(1.031-1.116)	<0.001	1.046(1.017-1.075)	0.002
PUSL1	1.026(1.012-1.041)	<0.001	1.026(1.007-1.046)	0.008	1.005(0.989-1.022)	0.529
RPUSD1	1.019(1.005-1.034)	0.007	1.037(1.005-1.069)	0.024	1.003 (0.989-1.018)	0.637
RPUSD2	1.006(0.958-1.055)	0.823	1.030(0.939-1.130)	0.533	1.032(0.992-1.074)	0.119
RPUSD3	1.050(1.024-1.078)	<0.001	1.039(1.017-1.062)	<0.001	1.033(1.009-1.058)	0.006
Age	1.010(0.996-1.025)	0.174	1.003(0.973-1.034)	0.863	0.994(0.982-1.005)	0.280
Gender (M/F)	0.776(0.531-1.132)	0.188	0.536(0.287-0.998)	0.049	0.933(0.673-1.294)	0.679
Grade (G3-4/G1-2)	1.141(0.784-1.661)	0.490			1.151(0.841-1.574)	0.380
Stage (III-IV/I-II)	2.500(1.721-3.632)	<0.001	2.479(1.355-4.533)	0.003	2.213(1.596-3.068)	<0.001

cases. Meanwhile, the expression of *DKC1*, *PUS7*, and *RPUSD1* was also higher in patients with advanced HCC (Supplementary Figure S1C). And the correlation between *PUSs* expression and tumor stage was also confirmed in the

LIRI-JP cohort (Supplementary Figure S1D). These results suggested that *PUSs* may be involved in the progression of HCC and may be associated with poor prognosis.

TABLE 2 Results of multivariate Cox analysis for *PUSs*.

Multivariate analysis						
Characteristics	Overall Survival (OS)				Progression Free Survival (PFS)	
	TCGA-LIHC		LIRI-JP		TCGA-LIHC	
	HR (95% CI)	<i>P</i>	HR (95% CI)	<i>P</i>	HR (95% CI)	<i>P</i>
DKC1	1.019(1.009-1.028)	<0.001	1.018(1.009-1.026)	<0.001	1.008(0.999-1.017)	0.076
PUS1	1.046(1.021-1.071)	<0.001	1.020(1.00 -1.036)	0.011	1.030(1.007-1.053)	0.010
PUS7	1.056(1.021-1.093)	0.002	1.066(1.024-1.110)	0.002	1.034(1.003-1.066)	0.031
PUSL1	1.018(1.003-1.033)	0.016	1.023(1.003-1.043)	0.024		
RPUSD1	1.012(0.998-1.027)	0.104	1.032(0.998-1.067)	0.064		
RPUSD3	1.041(1.015-1.067)	0.002	1.032(1.010-1.054)	0.004	1.029(1.005-1.054)	0.016

TABLE 3 Distribution of CNVs of *PUSs* and correlation of CNVs with *PUSs* expression in TCGA-LIHC.

Copy Number Variation of <i>PUSs</i> in TCGA-LIHC								
Gene	Total amplification (%)	Total deletion (%)	Heterozygous amplification (%)	Heterozygous deletion (%)	Homozygous amplification (%)	Homozygous deletion (%)	Spearman correlation	FDR
DKC1	23.24	17.57	21.35	17.30	1.89	0.27	0.17	0.002
PUS1	12.70	15.68	11.35	15.68	1.35	0.00	0.42	<0.001
PUS3	5.95	25.41	5.68	25.14	0.27	0.27	0.34	<0.001
PUS7	31.62	7.57	30.54	7.57	1.08	0.00	0.34	<0.001
PUS7L	12.97	10.81	12.70	10.81	0.27	0.00	0.28	<0.001
PUS10	12.43	9.73	12.16	9.46	0.27	0.27	0.30	<0.001
PUSL1	6.22	43.51	5.95	40.54	0.27	2.97	0.36	<0.001
RPUSD1	11.35	29.46	10.00	28.92	1.35	0.54	0.39	<0.001
RPUSD2	9.73	19.19	9.73	19.19	0.00	0.00	0.43	<0.001
RPUSD3	14.05	12.70	12.70	12.70	1.35	0.00	0.36	<0.001
RPUSD4	6.22	25.68	5.95	25.41	0.27	0.27	0.39	<0.001
TRUB1	9.73	28.65	9.73	28.65	0.00	0.00	0.30	<0.001
TRUB2	7.84	30.81	7.30	30.81	0.54	0.00	0.52	<0.001

Prognostic value of *PUSs* in hepatocellular carcinoma

First, we divided all HCC patients into high and low expression groups according to the median level of *PUSs* expression, and analyzed the survival differences between the two groups using the Kaplan-Meier method. As shown in Figures 3A,B, the patients with high expression of *DKC1*, *PUS1*, *PUS7*, *PUSL1*, and *RPUSD3* had better OS. And the same difference was also found in the PFS of patients (Figure 3C).

Then, Cox regression models were used for independent prognostic analysis. We included the four most common clinical features (age, gender, tumor stage, and tumor grade) as confounding

factors and excluded the patients who lacked complete clinical information. As a result, a total of 344 patients from the TCGA-LIHC cohort and 228 patients from the LIRI-JP cohort were included in the independent prognostic analysis, respectively (Supplementary Table S4). The univariate analysis showed that *DKC1*, *PUS1*, *PUS7*, *PUSL1*, *RPUSD1*, and *RPUSD3* were associated with poor OS and *DKC1*, *PUS1*, *PUS7*, and *RPUSD3* were associated with poor PFS (Table 1). Further multivariate analysis showed that *DKC1*, *PUS1*, *PUS7*, *PUSL1*, and *RPUSD3* were independent of the above clinical features, and could be used as independent risk factors for OS (Supplementary Figure S2). Meanwhile, *PUS1*, *PUS7*, and *RPUSD3* could be used as independent risk factors for PFS (Supplementary Figure S3).

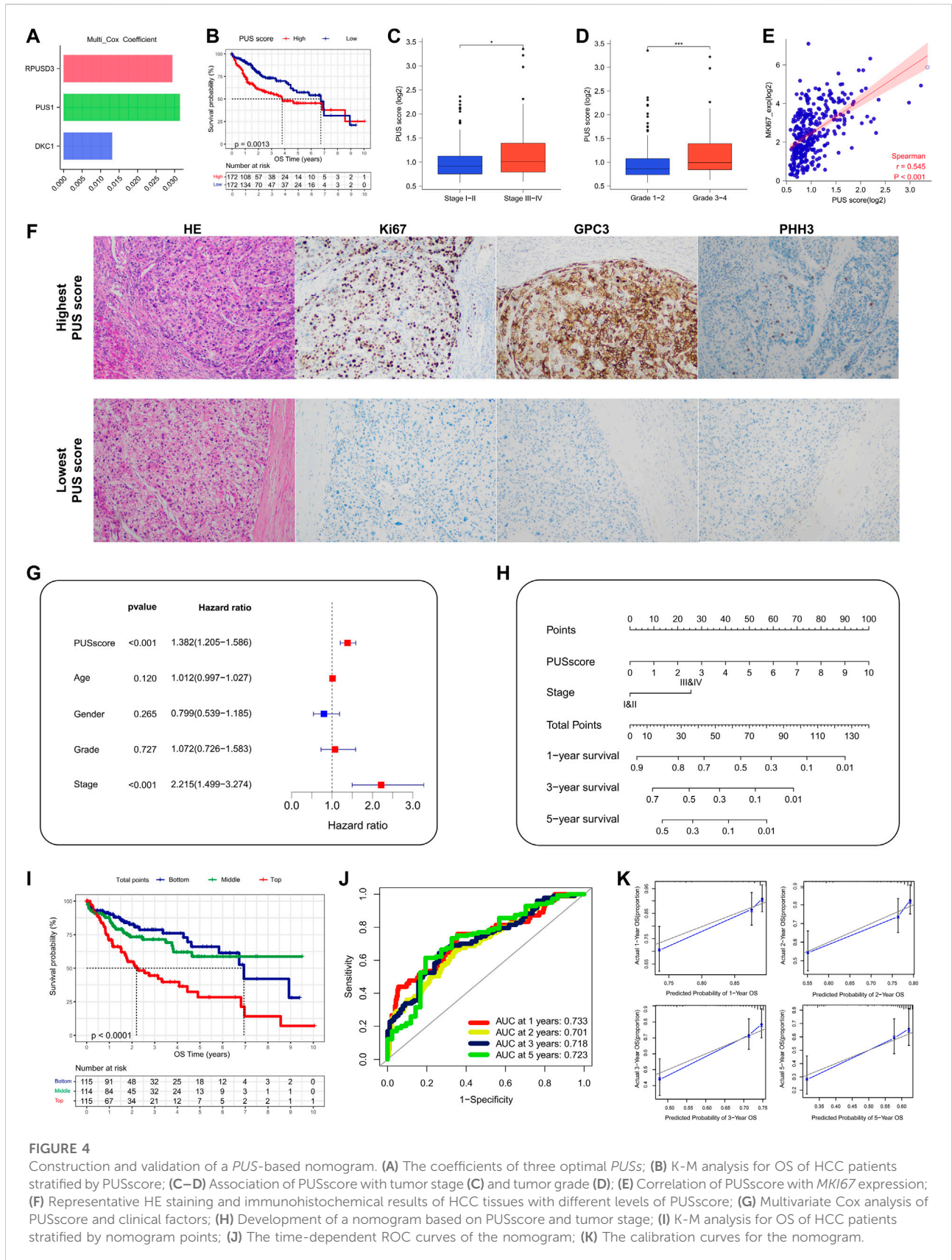
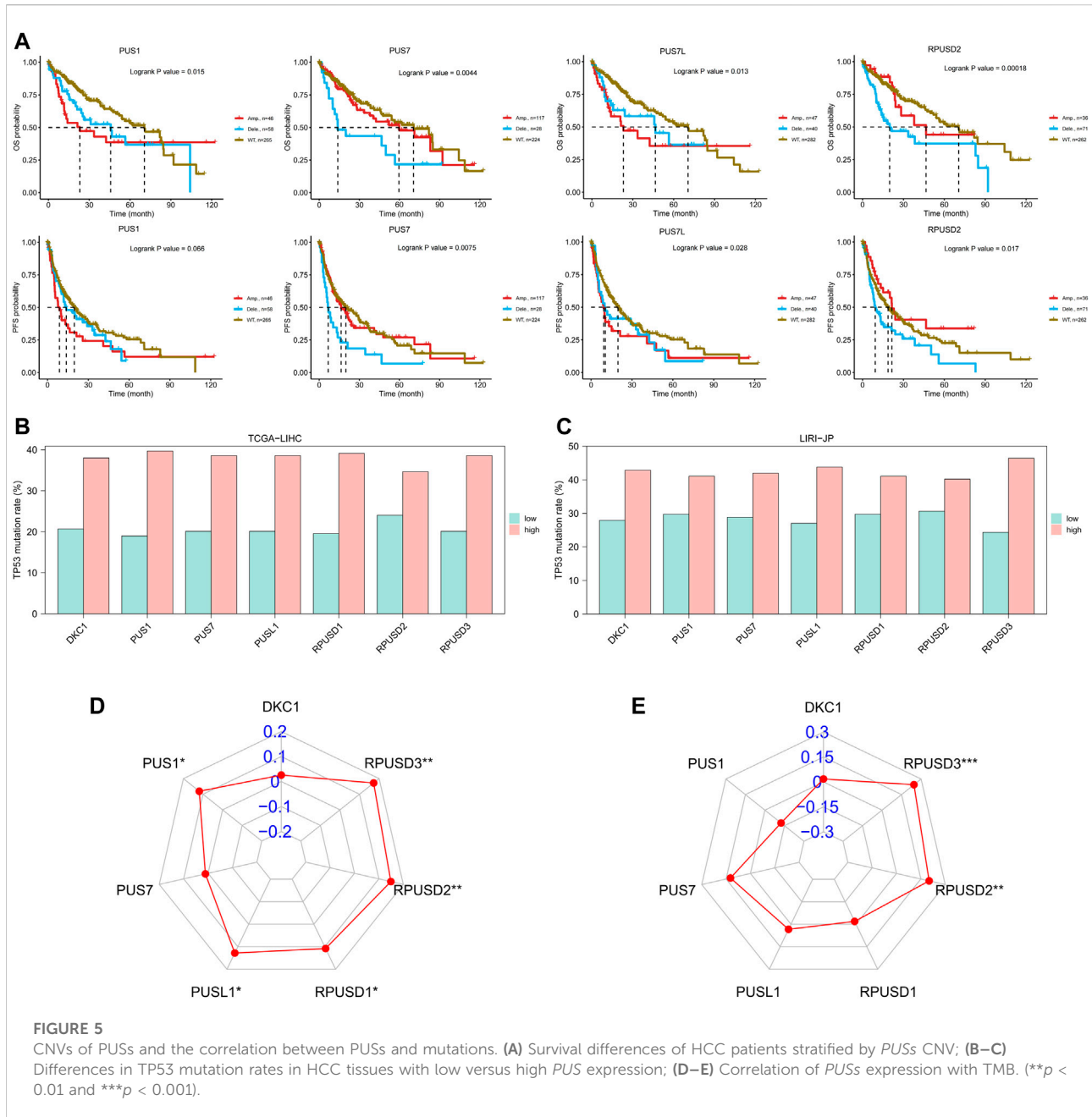


FIGURE 4

Construction and validation of a PUS-based nomogram. (A) The coefficients of three optimal PUSs; (B) K-M analysis for OS of HCC patients stratified by PUSscore; (C–D) Association of PUSscore with tumor stage (C) and tumor grade (D); (E) Correlation of PUSscore with MKI67 expression; (F) Representative HE staining and immunohistochemical results of HCC tissues with different levels of PUSscore; (G) Multivariate Cox analysis of PUSscore and clinical factors; (H) Development of a nomogram based on PUSscore and tumor stage; (I) K-M analysis for OS of HCC patients stratified by nomogram points; (J) The time-dependent ROC curves of the nomogram; (K) The calibration curves for the nomogram.

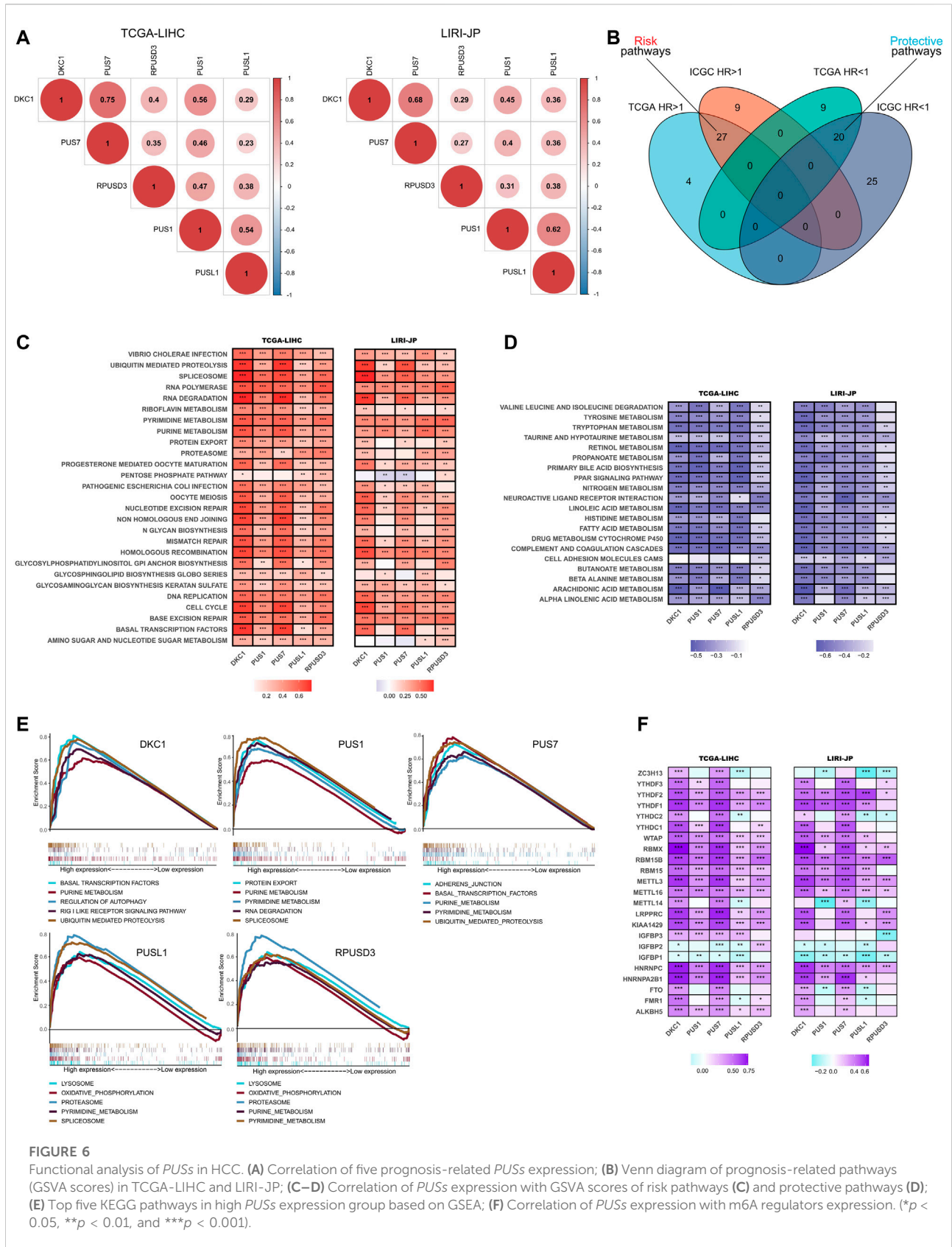


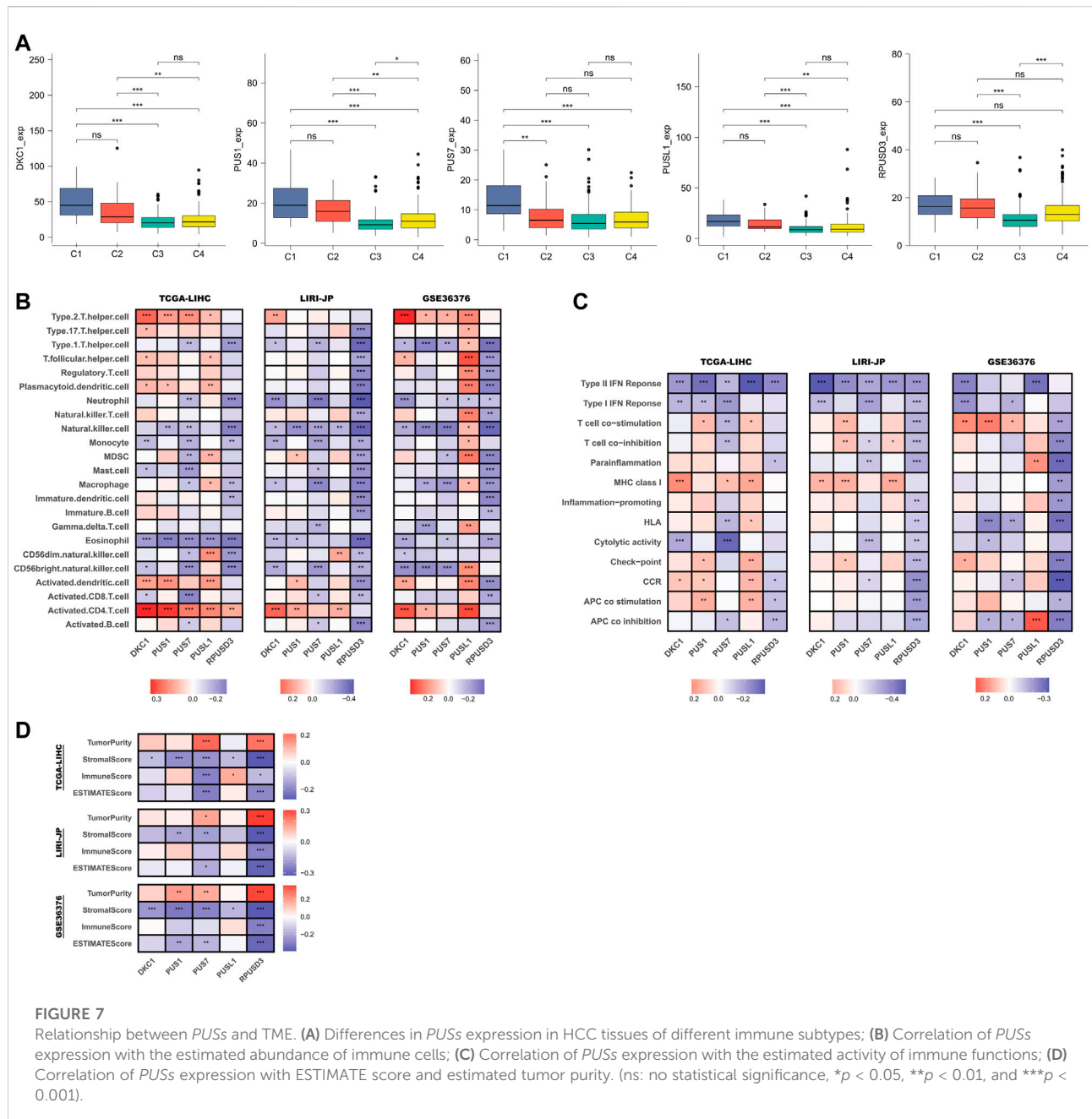
The hazard ratio and 95%CI adjusted by four clinical features were summarized in Table 2. Finally, we validated the expression of these five prognosis-related *PUSs* in clinical tissues and cell lines. As expected, their expression was consistently higher in HCC tissues than in non-cancerous tissues and in HCC cells (Hep3B and Huh7) than in LO2 cells. Besides, the results from the CCLE database (<https://portals.broadinstitute.org/ccle/about>) showed that these five *PUSs*' expression varied between different hepatocellular carcinoma cell lines (Supplementary Figure

S4). These results again demonstrated that *PUSs* might be closely related to HCC.

Establishment of a prognostic nomogram based on *PUSs*

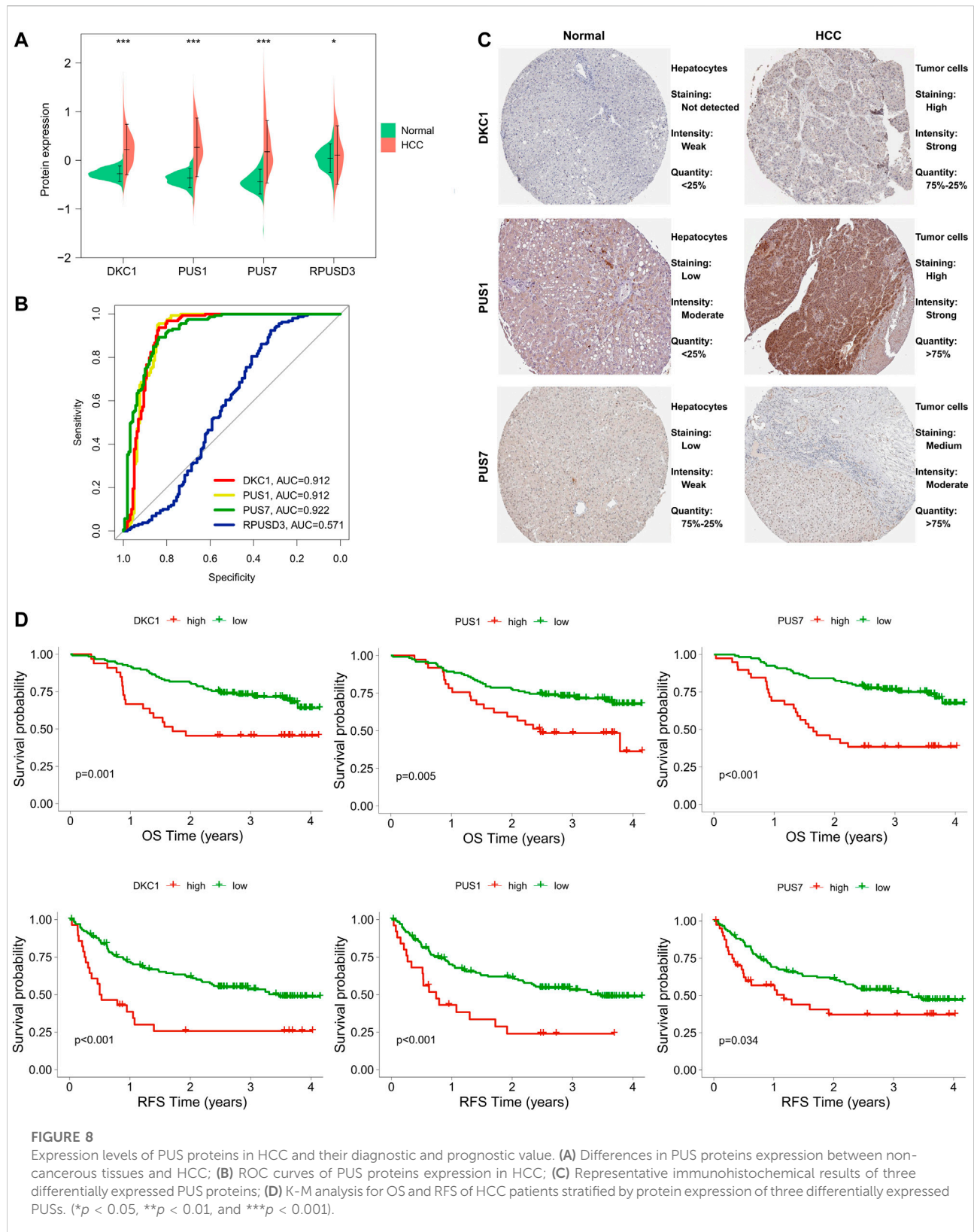
To apply the prognostic value of *PUSs* to clinical practice, we further constructed a nomogram using TCGA-LIHC data to predict OS.





First, based on the *PUSs* screened in the univariate analysis, we used multivariate COX analysis again to construct a *PUS*-related prognostic signature, which was calculated as follows: $PUS\ score = \sum(Exp_i * coef_i)$. Where Exp_i and $Coef_i$ denote the expression of *PUSs* and the coefficients obtained from multivariate COX analysis, respectively. The coefficients of the 3 *PUSs* in the signature are shown in Figure 4A. As expected, the patients with high *PUS* scores had poorer OS (Figure 4B). And the *PUS* score also correlated with the patient's tumor stage and grade (Figures 4C,D). Besides, we also observed a significant

positive correlation between the *PUS* score and the expression of *MKI67*, the encoding gene of *ki67* protein, which is one of the most commonly used prognostic indicators of malignancy in clinical practice (Figure 4E). We then calculated the relative *PUS* scores for the tissues from our clinical center based on the relative expression of *PUSs*. As shown in Figure 4F, the expression of *ki67* was significantly higher in the tissue with the highest *PUS* score than in that with the lowest *PUS* score. Further multivariate COX analysis showed that the signature was an independent prognostic factor for OS (Figure 4G). Next, we integrated the



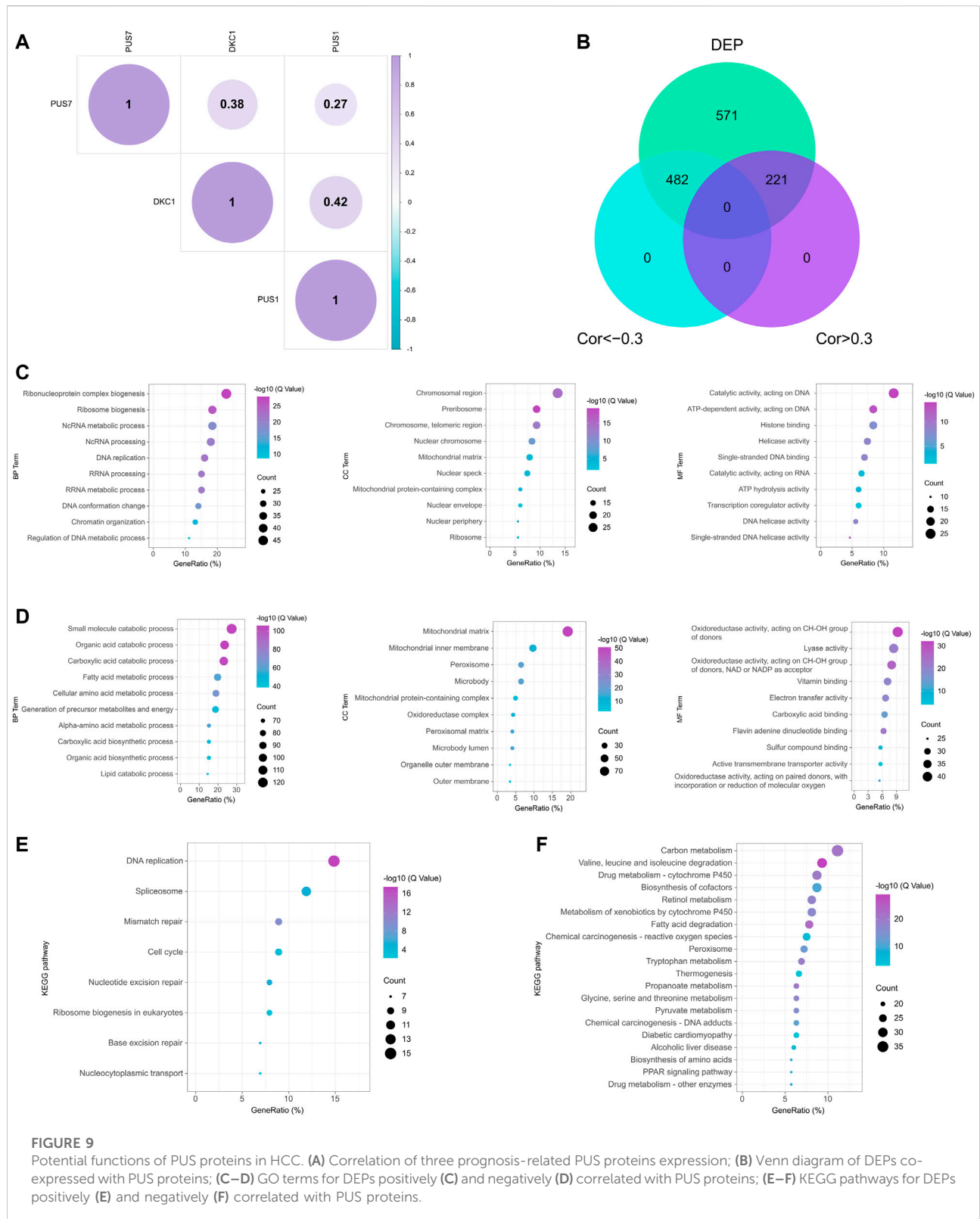


FIGURE 9 Potential functions of PUS proteins in HCC. **(A)** Correlation of three prognosis-related PUS proteins expression; **(B)** Venn diagram of DEPs co-expressed with PUS proteins; **(C–D)** GO terms for DEPs positively **(C)** and negatively **(D)** correlated with PUS proteins; **(E–F)** KEGG pathways for DEPs positively **(E)** and negatively **(F)** correlated with PUS proteins.

PUS score with another prognostic factor, the tumor stage, to establish a nomogram (Figure 4H). With this nomogram, we can calculate the risk score for patients and thus predict their OS. Then, we divided all patients into three groups based on their risk scores, and the K-M curves showed significant differences in OS between the three groups (Figure 4I). The ROC curves showed good accuracy for this nomogram in predicting OS with the AUC was 0.733 for 1-year, 0.701 for 2-year, 0.718 for 3-year and 0.723 for 5-year (Figure 4J), and the calibration curves showed the predictions were almost identical to the actual observations (Figure 4K). These results suggested that the nomogram was a robust prognostic predictor for patients in the TCGA-LIHC cohort. Finally, we validated the above findings in the LIRI-JP cohort (Supplementary Figure S5).

Copy number variations of *PUSs* and the correlation between *PUSs* and gene mutations in hepatocellular carcinoma

Here, the CNVs of *PUSs* in the TCGA-LIHC cohort were analyzed by using the GSCA database. First, we obtained the composition of *PUSs* CNVs. As can be seen in Table 3, the proportion of heterozygous CNV was significantly higher than that of homozygous CNV. Among them, *PUS7* had the highest percentage of heterozygous amplification, while *PUSL1* had the highest percentage of heterozygous deletion. Moreover, CNVs of *PUSs* were positively correlated with the mRNA expression of *PUSs*. Then, we analyzed the correlation between CNVs and patients' prognosis. As a result, CNV of four genes (*PUS1*, *PUS7*, *PUS7L*, and *RPUSD2*) were associated with patients' prognosis (Figure 5A). Of these, the deletion of *PUS7* and *RPUSD2* copy numbers mean poor OS and PFS. Patients with *PUS1* amplification had the worst OS, and patients with wild type of *PUS1* copy number had the best OS. As for *PUS7L*, its CNV was also associated with a poor prognosis. In detail, compared to *PUS7L* deletion, patients with *PUS7L* amplification had worse OS, but the difference was not significant in PFS. The above results suggested that the CNVs of *PUSs* may also be potential prognostic markers for HCC patients.

Due to the extremely low incidence of *PUSs* mutation in both HCC cohorts, we did not further analyze its significance. However, we noted a correlation between *PUSs* expression and mutations in *TP53*, the most mutated gene in both HCC cohorts (Supplementary Table S5). Based on the median of 7 DEGs expression, we divided all patients into high and low expression groups. Then we found a higher incidence of *TP53* mutation in the high expression group (Figures 5B,C). We also calculated the TMB of each HCC sample based on the somatic mutation data and found that the expression of *RPUSD2* and *RPUSD3* was positively correlated with TMB (Supplementary Table S6) (Figures 5D,E).

Potential pathways for the roles of *PUSs* in hepatocellular carcinoma

To further explore the roles of 5 independent prognostic *PUSs* in HCC, we performed functional pathway analyses based on two RNA-seq cohorts.

First, we analyzed the correlation between the 5 *PUSs* expression in HCC tissues. As shown in Figure 6A, the expression of these five genes was significantly positively correlated, suggesting that they may act synergistically with each other in HCC.

Next, we performed GSEA to evaluate the enrichment score of 186 KEGG pathways in each HCC sample and used univariate COX models to screen for prognosis-related pathways. As a result, we identified 31 risk pathways ($HR > 1$, $p < 0.05$) and 29 protective pathways ($HR < 1$, $p < 0.05$) in the TCGA-LIHC cohort, 36 risk pathways and 45 protective pathways in the LIRI-JP cohort (Supplementary Tables S7, S8). Moreover, 27 risk pathways and 20 protective pathways were filtered as the intersection of two results (Figure 6B). In detail, the risk pathways mainly focused on genetic information processing, substance metabolism, cell cycle, and immune response. And the protective pathways were almost entirely involved in metabolism.

Then, we analyzed the correlation between *PUSs* expression and the enrichment scores of these prognostic KEGG pathways. As expected, the expression of *PUSs* was significantly positively correlated with most risk pathways and negatively correlated with most protective pathways (Figures 6C,D). It was evident that *PUSs* may play broad roles in HCC and lead to poor clinical outcomes. Moreover, we also used GSEA to explore the KEGG pathways that were significantly enriched in samples with high *PUSs* expression (Supplementary Table S9). And the top 5 pathways ranked by NES for each *PUSs* are shown in Figure 6E. Consistent with previous results, many risk pathways were significantly enriched in samples with high *PUSs* expression. In addition, more pathways have been uncovered, including regulation of autophagy, RIG-I-like receptor pathway, adherens junction, lysosome, and oxidative phosphorylation. It can be seen that the relevance of *PUSs* to these pathways cannot be ignored.

Finally, we analyzed the correlation of *PUSs* with m6A, another post-transcriptional modification that is currently being studied with great fervor. As shown in Figure 6F, *PUSs* were significantly correlated with m6A-related genes, which suggested a link between two types of RNA modification, ψ and m6A, in HCC.

Relationship between *PUSs* and tumor microenvironment

First, we compared the differences in *PUSs* expression in samples of different immune subtypes. In the TCGA-LIHC

cohort, there were no samples classified as C5 subtype and, only 1 sample was classified as the C6 subtype (Supplementary Table S10). Therefore, we only compared samples of C1-4 subtypes. As shown in Figure 7A, PUSs expression was highest in HCC tissues of the C1 subtype (wound healing), followed by the C2 subtype (IFN- γ dominant). In contrast, PUSs expression was lowest in HCC tissues of the C3 subtype (inflammatory). These results suggested that PUSs may be associated with the tumor immune microenvironment. Next, we analyzed the correlation between the expression of PUSs and immune cells and immune pathways (Supplementary Tables S11, S12). The results in Figure 7B showed that PUSs were associated with multiple immune cell types. For example, the expression of *DKC1*, *PUS1*, and *PUSL1* was positively correlated with the abundance of activated CD4⁺ T cells, *DKC1* expression was positively correlated with Th2 cell, and the expression of *PUS1*, *PUS7*, and *RPUSD3* was negatively correlated with NK cell, etc. Meanwhile, we found that *RPUSD3* was negatively correlated with most of the immune cell types. In addition, PUSs were also associated with some immune functions, such as IFN response, T cell co-stimulation (Figure 7C). Notably, *RPUSD3* was also negatively associated with multiple immune functions. Then, we performed the ESTIMATE algorithm to analyze the correlation between PUSs and TME (Supplementary Table S13). As shown in Figure 7D, the expression of *PUS1* and *PUS7* was negatively correlated with the stromal score. *RPUSD3* expression was negatively correlated with both stromal and immune scores and positively correlated with tumor purity. Similar to *RPUSD3*, the expression of *PUS7* may also imply higher tumor purity.

Protein expression of PUSs in hepatocellular carcinoma and their diagnostic and prognostic value

To further explore the role of PUSs in HCC, we also assessed their value at the protein level.

First, we compared the differences in protein expression levels of these five PUSs in HCC tissues and normal tissues. As a result, four proteins (*DKC1*, *PUS1*, *PUS7*, and *RPUSD3*) were differentially expressed in the two groups of samples (Figure 8A). Notably, in the raw proteomics data, *PUSL1* did not pass the quality control criteria for the data and was therefore excluded from the analysis. To ensure the rigour of the study, we verified the results of PUS protein expression using the UALCAN database (<http://ualcan.path.uab.edu/>). As expected, *DKC1*, *PUS1*, *PUS7* and *RPUSD3* were significantly upregulated in HCC tissues. In contrast, *PUSL1* expression was not significantly different in HCC and normal tissues (Supplementary Figure S6). Next, we evaluated the diagnostic value of these 4 PUSs using ROC curves and found that *DKC1*, *PUS1*, and *PUS7* (AUC of 0.912, 0.912 and 0.922, respectively) could serve as diagnostic markers for HCC (Figure 8B). The above results suggested

that *DKC1*, *PUS1*, and *PUS7* were closely associated with HCC. Then, we obtained the representative immunohistochemical results from the HPA database, which also confirmed the higher expression of these 3 PUSs in HCC specimens than in normal liver specimens (Figure 8C). Finally, we analyzed the correlation between 3 PUSs and patients' prognosis using K-M curves. We divided the patients from the CPTAC cohort into two groups according to the best cut-off value of PUSs expression and found that patients in high expression groups had worse OS and RFS (Figure 8D).

Taken together, *DKC1*, *PUS1*, and *PUS7* were closely related to HCC and may serve as potential biomarkers for the diagnosis and prognosis of HCC.

Functional enrichment analysis of the PUSs co-expression network

Here, we explored the roles of PUSs in HCC. First, correlation analysis showed that *DKC1*, *PUS1*, and *PUS7* were co-expressed (Figure 9A). Consistent with the results at the mRNA level, they may play synergistic roles in HCC. Next, we screened for proteins associated with these 3 PUSs. In the CPTAC cohort, we found 1,274 DEPs using fold change >1.5 as the threshold. After that, we used the correlation coefficient to measure their correlation with the PUSs, with $|r| > 0.3$ being considered significant. As a result, 482 proteins negatively associated with PUSs expression and 221 positively associated with PUSs expression were identified, respectively (Figure 9B). Finally, we analyzed the GO terms and KEGG pathways enriched by these proteins (Supplementary Table S14). The count of enriched genes was used as the ranking criterion, and the top 10 GO terms for both groups of proteins were shown in Figures 9C,D, and the top 20 KEGG pathways were shown in Figures 9E,F. The results showed that the proteins positively associated with PUSs mainly function in genetic information processing (such as DNA replication and damage repair, transcription, and translation) and the cell cycle. Meanwhile, the proteins negatively associated with PUSs mainly function in metabolism. These results were almost identical to those at the mRNA level, which suggested that PUSs may affect HCC precisely by regulating these functions or pathways and gave us an initial insight into the role of PUSs in HCC.

Discussion

Pseudouridine (ψ) was the first post-transcriptional modification discovered and is one of the most abundant RNA modification types (Charette and Gray, 2000). Alterations in its deposition are involved in human diseases, including cancers (Nombela et al., 2021). For example, high levels of ψ have been detected in body fluids of patients with colon, prostate, ovarian and oral squamous cell carcinomas, suggesting

that ψ could be a potential biomarker for cancer diagnosis (Jiang et al., 2015; Krstulja et al., 2017; Sridharan et al., 2019; Stockert et al., 2019; Zeleznik et al., 2020). This has led to an increasing interest in the role of its modifying enzymes in cancer. Unsurprisingly, PUS is indeed associated with many human cancer types (Nombela et al., 2021). However, few studies have explored the role of PUS in HCC. To fill this scientific gap, our study integrated transcriptomic, proteomic and genomic data from HCC patients and confirmed the importance of PUS in HCC.

Previous studies have found that both protein and mRNA expression of *DKC1* was higher in HCC than in non-cancerous liver tissues and was associated with advanced clinical stage and poor prognosis (Liu et al., 2012; Ko et al., 2018; Zhang et al., 2021b; Li et al., 2022a). As for RNA-independent PUSs, their roles in HCC have rarely been explored. A previous study constructed a lactate metabolism-related gene signature to predict the prognosis of HCC patients, and *PUS1* was a key risk factor in this gene signature (Li et al., 2022b). To our knowledge, this is the only study that explores the value of RNA-independent PUSs in HCC. In our study, we found that seven PUS genes (*DKC1*, *PUS1*, *PUS7*, *PUSL1*, *RPUSD1*, *RPUSD2*, and *RPUSD3*) were significantly upregulated in HCC and they were expressed at higher levels in advanced stage or poorly differentiated HCC tissues. Importantly, all these 7 PUSs can be used as diagnostic markers for HCC, and 5 of them (*DKC1*, *PUS1*, *PUS7*, *PUSL1*, and *RPUSD3*) were risk factors for patients' survival independently of age, gender, stage and grade. Moreover, the protein levels of *DKC1*, *PUS1*, and *PUS7* were also significantly upregulated in HCC and associated with poor prognosis. Our findings filled a gap where most PUSs have been left unstudied in HCC and confirmed the involvement of PUSs in HCC. The nomogram we further constructed also applied the prognostic value of PUSs to the clinic, providing clinicians with a guide that can accurately predict patient prognosis.

As for the molecular mechanism of PUS involvement in cancer, it has been reported that overexpression of *DKC1* increased the expression of TERC and rRNA pseudouridylation, promoting the proliferation of colorectal cancer (Turano et al., 2008; Nersisyan et al., 2019). The upregulation of *PUS7* promoted CRC cell metastasis and was independent of the catalytic activity of *PUS7*. This mean *PUS7*-mediated ψ may not govern the metastatic capacity of CRC cells. Meanwhile, the HSP90/*PUS7*/*LASP1* axis was a potential mechanism by which *PUS7* promoted CRC metastasis (Song et al., 2021). Another study showed that *PUS7* could promote CRC cell proliferation and invasion by activating PI3K/AKT/mTOR signaling pathway (Du et al., 2021). In glioma, *DKC1* up-regulation was common and necessary for extensive tumor growth. *DKC1* could upregulate the expression of N-cadherin, MMP-2, HIF1A, CDK2, and cyclin E, and the glioma cells with *DKC1* knockdown exhibited low motility. Meanwhile, *DKC1* knockdown also altered the expression of cell cycle-relative molecules to arrest at the G1 phase (Miao et al., 2022). Moreover,

the molecular mechanisms of *PUS1* involvement in melanoma and breast cancer, and *PUS10* involvement in prostate cancer have also been initially explored (Zhao et al., 2004; Jana et al., 2017).

So how is PUS involved in HCC? What functions are available? What pathways? Unfortunately, there has not been sufficient research to address these issues. As for some typical pathways with strong relevance to PUS in our study, abnormalities in cell cycle progression are one of the fundamental mechanisms of tumorigenesis. Cell cycle regulatory pathways are combined with other features of cancer, including metabolic remodelling and immune escape. This makes regulators of the cell cycle machinery a reasonable target for anti-cancer therapy (Liu et al., 2022). Meanwhile, the cell cycle is driven by the activation of cell cycle protein-dependent kinases (CDKs), whose activity is controlled by ubiquitin-mediated proteolysis of key regulators such as cell cycle proteins and CDK inhibitors (Nakayama and Nakayama, 2006). From this, we inferred that ubiquitin-mediated proteolysis may be closely related to the cell cycle, and they might synergistically or independently affect the prognosis of HCC patients. Next, we turn our attention to transcription-related pathways. The spliceosome is thought to be general cellular 'housekeeping' machinery. Spliceosomal mutations and aberrant splicing are also closely associated with human cancer. Also, some spliceosome gene mutations can lead to immune dysregulation. As a result, spliceosome-targeted therapies (STTs) have emerged as highly effective anti-cancer strategies (Yang et al., 2021). Transcription mediated by RNA polymerases is an important factor in determining the growth of cancer cells. However, inactivation of some tumor suppressors (e.g., p53) in cancer can dysregulate RNA polymerases, and oncoproteins (e.g., Myc) can further stimulate these systems. Such events may have a significant impact on the growth of cancer cells (White, 2005). And the basal transcription factors play a vital role in the initiation of transcription of the encoded genes. They are a group of protein molecules necessary for RNA polymerase to bind the promoter (Reese, 2003). As for DNA replication and damage repair, their involvement in cancer and as features of cancer is an accepted fact and therefore does not require more elaboration (Modrich, 1994; Gaillard et al., 2015; Jeggo et al., 2016; Carbone et al., 2020). Cancer is also a metabolic disease due to a metabolic disorder (Boroughs and DeBerardinis, 2015). Then HCC is destined to be inextricably linked to metabolic disorders, as the liver is the central metabolic organ of the body (Ng et al., 2017). The prognosis-related pathways derived in our study again supported the idea that metabolism may be another determinant of the impact of PUSs on HCC. Interestingly, the effect of PUSs on nucleotide metabolism appeared to be distinct from its effect on the metabolism of other substances, although they both ultimately lead to a poorer prognosis. Overall, the pathways regulated by PUSs in HCC are likely to be very broad and interconnected. And it is also unknown

whether these functions are dependent on the catalytic activity of PUS. In future, research should focus on the effect of PUS on the above pathways in HCC.

TME also plays crucial roles in the pathogenesis, malignant features, and treatment of HCC (Hernandez-Gea et al., 2013). Therefore, the link between PUSs and TME should also be considered. The correlation between cell cycle and immune response, the enrichment of immune-related pathways in GSEA, the differential expression of PUSs in different immune subtypes of tissues, the correlation between PUSs expression and immune cell infiltration as well as immune function, and the association of PUSs expression with the ESTIMAT score, they all suggested that PUSs may be potential regulators of TME. Among them, the expression of *RPUSD3* seemed to imply a lack of immune cells and a low level of many immune functions in the TME. This was supported by the positive correlation between its expression and tumor purity. So what does the association of PUSs with TME lead to? Some examples, it was found that NK cell was the main antitumor cell type in the liver (Sonnenberg and Hepworth, 2019). The IFN response plays crucial roles in promoting host antitumor immunity and is considered a critical component of the cancer elimination phase of cancer immunosurveillance (Dunn et al., 2006). Therefore, we hypothesized that the role of PUSs in HCC may be partly through influencing antitumor immunity. Nevertheless, the TME is very complex. Some ingredients can even have opposite effects under different conditions. The mechanisms by which PUSs shape the TME are yet to be further explored.

There is now consensus that mutation of TP53 converts it from a tumor suppressor gene to an oncogene. The mutated TP53 loses its original regulatory functions, which are mainly focused on cell cycle, apoptosis, DNA repair, etc. (Vaddavalli and Schumacher, 2022). This also coincides with the findings of our study. As for the CNV of PUSs, its impact on the prognosis of HCC patients has also been revealed. Hence, more emphasis should be placed on the CNV of PUSs in future.

Certain limitations of our study are to be acknowledged. First, due to data limitations, some critical risk factors, such as HBV infection, were not included in the analysis, which may have led to biased conclusions. Second, the proteomic analysis was based on only one Chinese HBV-related HCC cohort. Therefore, there is a need to further dissect the value of PUS proteins in a larger sample. Third, the molecular mechanisms underlying the role of PUSs in HCC need to be further investigated through comprehensive *in vivo* and *in vitro* experiments. We will continue to focus on these issues in future research.

Conclusion

In conclusion, multiple PUS genes expression was upregulated in HCC. Among them, *DKC1*, *PUS1*, *PUS7*, *PUSL1*, and *RPUSD3* were independent risk factors for OS. At the protein level, the expression of *DKC1*, *PUS1*, and *PUS7* was upregulated in HCC and correlated with

poor prognosis. Moreover, both mRNA expression and protein expression of PUSs were highly diagnostic of HCC. Further functional analysis revealed that PUSs might be involved in the regulation of multiple pathways in HCC. Therefore, PUSs may play essential roles in HCC and can be used as potential biomarkers for the diagnosis and prognosis of patients.

Data availability statement

The datasets presented in this study can be found in online repositories. The names of the repository/repositories and accession number(s) can be found in the article/Supplementary Material.

Ethics statement

The studies involving human participants were reviewed and approved by Qingdao Municipal Hospital Ethics Committee. The patients/participants provided their written informed consent to participate in this study.

Author contributions

ZJ, WZ, and GS designed the research. ZJ performed the experiments. ZJ, MS, JW, DS, and HL collected and analyzed the data. ZJ carried out the research and wrote the manuscript. WZ and GS reviewed the manuscript. GS supervised the study. All authors have read and approved the final version of the manuscript.

Acknowledgments

We sincerely thank all the developers of the databases and algorithms employed in our study.

Conflict of Interest

The authors declare that the research was conducted in the absence of any commercial or financial relationships that could be construed as a potential conflict of interest.

Publisher's note

All claims expressed in this article are solely those of the authors and do not necessarily represent those of their affiliated organizations, or those of the publisher, the editors and the reviewers. Any product that may be evaluated in this article, or claim that may be made by its

manufacturer, is not guaranteed or endorsed by the publisher.

Supplementary material

The Supplementary Material for this article can be found online at: <https://www.frontiersin.org/articles/10.3389/fgene.2022.944681/full#supplementary-material>

SUPPLEMENTARY FIGURE S1

Correlation between PUSs expression and clinicopathological parameters.

SUPPLEMENTARY FIGURE S2

Multivariate Cox analysis of PUSs mRNA and clinical factors for OS.

SUPPLEMENTARY FIGURE S3

Multivariate Cox analysis of PUSs mRNA and clinical factors for PFS.

SUPPLEMENTARY FIGURE S4

Relative expression of five prognosis-related PUSs in clinical tissues and cell lines.

SUPPLEMENTARY FIGURE S5

Validation of PUS score and nomogram in the LIRI-JP cohort.

SUPPLEMENTARY FIGURE S6

Results of differential analysis of PUS protein expression in the UALCAN database.

SUPPLEMENTARY TABLE S1

Thirteen pseudouridine synthases in human cells;

SUPPLEMENTARY TABLE S2

Primer sequences used for RT-qPCR.

SUPPLEMENTARY TABLE S3

Results of differential expression analysis of PUS mRNA.

SUPPLEMENTARY TABLE S4

Patients involved in multivariate Cox analysis.

SUPPLEMENTARY TABLE S5

TP53 mutation status of HCC samples.

SUPPLEMENTARY TABLE S6

TMB data of HCC patients.

SUPPLEMENTARY TABLE S7

GSVA scores of the KEGG pathways in HCC samples.

SUPPLEMENTARY TABLE S8

Univariate Cox analysis of KEGG pathways for OS.

SUPPLEMENTARY TABLE S9

GSEA results for high PUSs expression samples in TCGA-LIHC.

SUPPLEMENTARY TABLE S10

Immune subtype of HCC samples in TCGA-LIHC.

SUPPLEMENTARY TABLE S11

The annotated gene sets used in ssGSEA.

SUPPLEMENTARY TABLE S12

Results of ssGSEA.

SUPPLEMENTARY TABLE S13

Results of ESTIMATE.

SUPPLEMENTARY TABLE S14

Results of the functional enrichment analysis of proteins.

References

- Barbie, D. A., Tamayo, P., Boehm, J. S., Kim, S. Y., Moody, S. E., Dunn, I. F., et al. (2009). Systematic RNA interference reveals that oncogenic KRAS-driven cancers require TBK1. *Nature* 462 (7269), 108–112. doi:10.1038/nature08460
- Becht, E., Giraldo, N. A., Lacroix, L., Buttard, B., Elarouci, N., Petitprez, F., et al. (2016). Estimating the population abundance of tissue-infiltrating immune and stromal cell populations using gene expression [published correction appears in *Genome Biol.* 2016 Dec 1;17 (1):249]. *Genome Biol.* 17 (1), 218. doi:10.1186/s13059-016-1070-5
- Boroughs, L. K., and DeBerardinis, R. J. (2015). Metabolic pathways promoting cancer cell survival and growth. *Nat. Cell Biol.* 17 (4), 351–359. doi:10.1038/ncb3124
- Carbone, M., Arron, S. T., Beutler, B., Bononi, A., Cavenee, W., Cleaver, J. E., et al. (2020). Tumour predisposition and cancer syndromes as models to study gene-environment interactions. *Nat. Rev. Cancer* 20 (9), 533–549. doi:10.1038/s41568-020-0265-y
- Charette, M., and Gray, M. W. (2000). Pseudouridine in RNA: What, where, how, and why. *IUBMB Life* 49 (5), 341–351. doi:10.1080/152165400410182
- Cui, Q., Yin, K., Zhang, X., Ye, P., Chen, X., Chao, J., et al. (2021). Targeting PUS7 suppresses tRNA pseudouridylation and glioblastoma tumorigenesis. *Nat. Cancer* 2 (9), 932–949. doi:10.1038/s43018-021-00238-0
- Delaunay, S., and Frye, M. (2019). RNA modifications regulating cell fate in cancer. *Nat. Cell Biol.* 21 (5), 552–559. doi:10.1038/s41568-019-0319-0
- Du, J., Gong, A., Zhao, X., and Wang, G. (2021). Pseudouridylate synthase 7 promotes cell proliferation and invasion in colon cancer through activating PI3K/AKT/mTOR signaling pathway. *Dig. Dis. Sci.* 67, 1260–1270. doi:10.1007/s10620-021-06936-010.1007/s10620-021-06936-0
- Dunn, G. P., Koebel, C. M., and Schreiber, R. D. (2006). Interferons, immunity and cancer immunoeediting. *Nat. Rev. Immunol.* 6 (11), 836–848. doi:10.1038/nri1961
- Gaillard, H., García-Muse, T., and Aguilera, A. (2015). Replication stress and cancer. *Nat. Rev. Cancer* 15 (5), 276–289. doi:10.1038/nrc3916
- Gao, Q., Zhu, H., Dong, L., Shi, W., Chen, R., Song, Z., et al. (2019). Integrated proteogenomic characterization of HBV-related hepatocellular carcinoma. *Cell* 179 (2), 1240561–1240577. e22. doi:10.1016/j.cell.2019.08.052
- Hänzelmann, S., Castelo, R., and Guinney, J. (2013). Gsva: Gene set variation analysis for microarray and RNA-seq data. *BMC Bioinforma.* 14 (7), 7. doi:10.1186/1471-2105-14-7
- Hernandez-Gea, V., Toffanin, S., Friedman, S. L., and Llovet, J. M. (2013). Role of the microenvironment in the pathogenesis and treatment of hepatocellular carcinoma. *Gastroenterology* 144 (3), 512–527. doi:10.1053/j.gastro.2013.01.002
- Jana, S., Hsieh, A. C., and Gupta, R. (2017). Reciprocal amplification of caspase-3 activity by nuclear export of a putative human RNA-modifying protein, PUS10 during TRAIL-induced apoptosis. *Cell Death Dis.* 8 (10), e3093. Published 2017 Oct 5. doi:10.1038/cddis.2017.476
- Jeggo, P. A., Pearl, L. H., and Carr, A. M. (2016). DNA repair, genome stability and cancer: A historical perspective. *Nat. Rev. Cancer* 16 (1), 35–42. doi:10.1038/nrc.2015.4
- Jiang, T., Lin, Y., Yin, H., Wang, S., Sun, Q., Zhang, P., et al. (2015). Correlation analysis of urine metabolites and clinical staging in patients with ovarian cancer. *Int. J. Clin. Exp. Med.* 8 (10), 18165–18171.
- Jonkhout, N., Tran, J., Smith, M. A., Schonrock, N., Mattick, J. S., and Novoa, E. M. (2017). The RNA modification landscape in human disease. *RNA* 23 (12), 1754–1769. doi:10.1261/rna.063503.117
- Kan, G., Wang, Z., Sheng, C., Chen, G., Yao, C., Mao, Y., et al. (2021). Dual inhibition of DKC1 and MEK1/2 synergistically restrains the growth of colorectal cancer cells. *Adv. Sci.* 8 (10), 2004344. Published 2021 Mar 15. doi:10.1002/adv.202004344
- Ko, E., Kim, J. S., Ju, S., Seo, H. W., Chang, Y., Kang, J. A., et al. (2018). Oxidatively modified protein-disulfide isomerase-associated 3 promotes Dyskerin pseudouridine synthase 1-mediated malignancy and survival of hepatocellular carcinoma cells. *Hepatology* 68 (5), 1851–1864. doi:10.1002/hep.30039
- Krstulja, A., Lettieri, S., Hall, A. J., Roy, V., Favetta, P., and Agrofoglio, L. A. (2017). Tailor-made molecularly imprinted polymer for selective recognition of the urinary tumor marker pseudouridine. *Macromol. Biosci.* 17 (12), 1700250. doi:10.1002/mabi.20170025010.1002/mabi.201700250

- Li, H., Chen, L., Han, Y., Zhang, F., and Wang, Y. (2021). The identification of RNA modification gene *PUS7* as a potential biomarker of ovarian cancer. *Biol. (Basel)* 10 (11), 1130. doi:10.3390/biology10111130
- Li, L., Cao, Y., Fan, Y., and Li, R. (2022). Gene signature to predict prognostic survival of hepatocellular carcinoma. *Open Med. (Wars)* 17 (1), 135–150. Published 2022 Jan 7. doi:10.1515/med-2021-0405
- Li, X., Ma, S., and Yi, C. (2016). Pseudouridine: The fifth RNA nucleotide with renewed interests. *Curr. Opin. Chem. Biol.* 33, 108–116. doi:10.1016/j.cbpa.2016.06.014
- Li, Y., Mo, H., Wu, S., Liu, X., and Tu, K. (2022). A novel lactate metabolism-related gene signature for predicting clinical outcome and tumor microenvironment in hepatocellular carcinoma. *Front. Cell Dev. Biol.* 9, 801959. Published 2022 Jan 3. doi:10.3389/fcell.2021.801959
- Liu, B., Zhang, J., Huang, C., and Liu, H. (2012). Dyskerin overexpression in human hepatocellular carcinoma is associated with advanced clinical stage and poor patient prognosis. *PLoS One* 7 (8), e43147. doi:10.1371/journal.pone.0043147
- Liu, C. J., Hu, F. F., Xia, M. X., Han, L., Zhang, Q., and Guo, A. Y. (2018). GSCALite: A web server for gene set cancer analysis. *Bioinformatics* 34 (21), 3771–3772. doi:10.1093/bioinformatics/bty411
- Liu, J., Peng, Y., and Wei, W. (2022). Cell cycle on the crossroad of tumorigenesis and cancer therapy. *Trends Cell Biol.* 32 (1), 30–44. doi:10.1016/j.tcb.2021.07.001
- Llovet, J. M., Kelley, R. K., Villanueva, A., Singal, A. G., Pikarsky, E., Roayaie, S., et al. (2021). Hepatocellular carcinoma. *Nat. Rev. Dis. Prim.* 7 (16), 6. doi:10.1038/s41572-020-00240-3
- Llovet, J. M., Montal, R., Sia, D., and Finn, R. S. (2018). Molecular therapies and precision medicine for hepatocellular carcinoma. *Nat. Rev. Clin. Oncol.* 15 (10), 599–616. doi:10.1038/s41571-018-0073-4
- Miao, F. A., Chu, K., Chen, H. R., Zhang, M., Shi, P. C., Bai, J., et al. (2022). Increased DKC1 expression in glioma and its significance in tumor cell proliferation, migration and invasion. *Invest. New Drugs* 37 (6), 1177–1186. doi:10.1007/s10637-019-00748-w
- Modrich, P. (1994). Mismatch repair, genetic stability, and cancer. *Science* 266 (5193), 1959–1960. doi:10.1126/science.7801122
- Nakayama, K. I., and Nakayama, K. (2006). Ubiquitin ligases: Cell-cycle control and cancer. *Nat. Rev. Cancer* 6 (5), 369–381. doi:10.1038/nrc1881
- Nersisyan, L., Hopp, L., Loeffler-Wirth, H., Galle, J., Loeffler, M., Arakelyan, A., et al. (2019). Telomere length maintenance and its transcriptional regulation in lynch syndrome and sporadic colorectal carcinoma. *Front. Oncol.* 9, 1172. doi:10.3389/fonc.2019.01172
- Ng, C. K. Y., Piscuoglio, S., and Terracciano, L. M. (2017). Molecular classification of hepatocellular carcinoma: The view from metabolic zonation. *Hepatology* 66 (5), 1377–1380. doi:10.1002/hep.29311
- Nombela, P., Miguel-López, B., and Blanco, S. (2021). The role of m6A, m5C and Ψ RNA modifications in cancer: Novel therapeutic opportunities. *Mol. Cancer* 20 (1), 18. doi:10.1186/s12943-020-01263-w
- Reese, J. C. (2003). Basal transcription factors. *Curr. Opin. Genet. Dev.* 13 (2), 114–118. doi:10.1016/s0959-437x(03)00013-3
- Roayaie, S., Obeidat, K., Sposito, C., Mariani, L., Bhoori, S., Pellegrinelli, A., et al. (2013). Resection of hepatocellular cancer ≤2 cm: Results from two western centers. *Hepatology* 57 (4), 1426–1435. doi:10.1002/hep.25832
- Roundtree, I. A., Evans, M. E., Pan, T., and He, C. (2017). Dynamic RNA modifications in gene expression regulation. *Cell* 169 (7), 1187–1200. doi:10.1016/j.cell.2017.05.045
- Song, D., Guo, M., Xu, S., Song, X., Bai, B., Li, Z., et al. (2021). HSP90-dependent PUS7 overexpression facilitates the metastasis of colorectal cancer cells by regulating LASP1 abundance. *J. Exp. Clin. Cancer Res.* 40 (1), 170. doi:10.1186/s13046-021-01951-5
- Sonnenberg, G. F., and Hepworth, M. R. (2019). Functional interactions between innate lymphoid cells and adaptive immunity. *Nat. Rev. Immunol.* 19 (10), 599–613. doi:10.1038/s41577-019-0194-8
- Sridharan, G., Ramani, P., Patankar, S., and Vijayaraghavan, R. (2019). Evaluation of salivary metabolomics in oral leukoplakia and oral squamous cell carcinoma. *J. Oral Pathol. Med.* 48 (4), 299–306. doi:10.1111/jop.12835
- Stockert, J. A., Gupta, A., Herzog, B., Yadav, S. S., Tewari, A. K., and Yadav, K. K. (2019). Predictive value of pseudouridine in prostate cancer. *Am. J. Clin. Exp. Urol.* 7 (4), 262–272.
- Subramanian, A., Tamayo, P., Mootha, V. K., Mukherjee, S., Ebert, B. L., Gillette, M. A., et al. (2005). Gene set enrichment analysis: A knowledge-based approach for interpreting genome-wide expression profiles. *Proc. Natl. Acad. Sci. U. S. A.* 102 (43), 15545–15550. doi:10.1073/pnas.0506580102
- Thorsson, V., Gibbs, D. L., Brown, S. D., Wolf, D., Bortone, D. S., Ou Yang, T. H., et al. (2019). The immune landscape of cancer. *Immunity* 5148 (24), 411812–412830. e14. doi:10.1016/j.immuni.2018.03.023
- Turano, M., Angrisani, A., De Rosa, M., Izzo, P., and Furia, M. (2008). Real-time PCR quantification of human DKC1 expression in colorectal cancer. *Acta Oncol.* 47 (8), 1598–1599. doi:10.1080/02841860801898616
- Uhlén, M., Fagerberg, L., Hallström, B. M., Lindskog, C., Oksvold, P., Mardinoglu, A., et al. (2015). Proteomics. Tissue-based map of the human proteome. *Science* 347 (6220), 1260419. doi:10.1126/science.1260419
- Vaddavalli, P. L., and Schumacher, B. (2022). The p53 network: Cellular and systemic DNA damage responses in cancer and aging. *Trends Genet.* S0168-9525 (22), 598–612. doi:10.1016/j.tig.2022.02.010
- White, R. J. (2005). RNA polymerases I and III, growth control and cancer. *Nat. Rev. Mol. Cell Biol.* 6 (1), 69–78. doi:10.1038/nrm1551
- Yang, H., Beutler, B., and Zhang, D. (2021). Emerging roles of spliceosome in cancer and immunity. *Protein Cell* 13, 559–579. doi:10.1007/s13238-021-00856-510.1007/s13238-021-00856-5
- Yang, J. D., Hainaut, P., Gores, G. J., Amadou, A., Plymoth, A., and Roberts, L. R. (2019). A global view of hepatocellular carcinoma: Trends, risk, prevention and management. *Nat. Rev. Gastroenterol. Hepatol.* 16 (10), 589–604. doi:10.1038/s41575-019-0186-y
- Zelznik, O. A., Eliassen, A. H., Kraft, P., Poole, E. M., Rosner, B. A., Jeanfavre, S., et al. (2020). A prospective analysis of circulating plasma metabolites associated with ovarian cancer risk. *Cancer Res.* 80 (6), 1357–1367. doi:10.1158/0008-5472.CAN-19-2567
- Zhang, D. Y., Ming, G. L., and Song, H. (2021a). PUS7: A targetable epitranscriptomic regulator of glioblastoma growth. *Trends Pharmacol. Sci.* 42 (12), 976–978. doi:10.1016/j.tips.2021.10.002
- Zhang, M., Zhao, W., Liu, S., Liu, H., Liu, L., Peng, Q., et al. (2021b). H/ACA snoRNP gene family as diagnostic and prognostic biomarkers for hepatocellular carcinoma. *Pharmgenomics. Pers. Med.* 14, 1331–1345. doi:10.2147/PGPM.S333838
- Zhao, X., Patton, J. R., Davis, S. L., Florence, B., Ames, S. J., and Spanjaard, R. A. (2004). Regulation of nuclear receptor activity by a pseudouridine synthase through posttranscriptional modification of steroid receptor RNA activator. *Mol. Cell* 15 (4), 549–558. doi:10.1016/j.molcel.2004.06.044